Investigation of metal-barrier-metal-barrier-metal structures

A. G. Aleksanyan, É. M. Belenov, I. N. Kompanets, Yu. M. Popov, I. A. Poluéktov,
S. I. Sagitov, E. M. Soboleva, A. G. Sobolev, A. V. Uskov, and V. G. Tsukanov

Lebedev Physical Institute, Academy of Sciences of the USSR
(Submitted 17 December 1981; resubmitted 6 May 1982)
Zh. Eksp. Teor. Fiz. **82**, 1389–1397 (October 1982)

A mechanism for obtaining segments with negative differential resistance on the current-voltage characteristic of a two-barrier metal-barrier-metal-barrier-metal (MBMBM) structure is proposed and experimental structures of this type have been constructed using Au and Al films as the metals and MgO and Al_2O_3 dielectric films as the barriers. Electromagnetic oscillations at 180 kHz, tunable over a range of 30 kHz, have been generated by the two-barrier experimental structures. The parameters for a frequency-tunable generator in the 10^9–10^{14} Hz range are calculated theoretically.

PACS numbers: 73.40.Rw

1. INTRODUCTION

Metal-barrier-metal (MBM) structures attract attention because of their manifold physical properties and the enormous range of their possible applications. In quantum and optical electronics, MBM junctions are used as uniquely fast detectors,[1] as "matrices" for investigating substances by tunnel spectroscopy,[2] as frequency multipliers and mixers of electromagnetic radiation in the microwave, infrared, and even the optical regions,[3–5] and as light amplifiers and sources.[6]

MBM junctions of two types are well known: point junctions which consist of the contact of a sharply pointed (to a radius of the order of 100 Å) metallic whisker with an oxidized metallic surface, and planar junctions, which consist of two narrow metallic bands deposited criss cross on a substrate, the lower band being oxidized. In both cases the barrier is a layer of the oxide of the corresponding metal, some 10–50 Å thick. The operation of these devices is based on the tunneling of electrons through the barrier from one metal piece to the other. This mechanism is essentially nonlinear,[7] and the differential resistance is different in different parts of the current-voltage curve (IVC). By placing the working point on the IVC in the region of greatest nonlinearity, one can obtain the diode effect necessary for detecting signals and can achieve frequency mixing as a result of the nonlinearity. Here we assume that the IVC retains its nonlinearity clear up to high frequencies (of the order of 10^{16} Hz).[8] The validity of these assumptions is confirmed by the successful results of an experimental study of the interaction of MBM detectors and mixers with electromagnetic radiation.[4] No other known device has such rapid action.

The interest in the nonlinear properties of MBM structures has recently risen sharply in view of the possibility of obtaining negative differential resistance (NDR) on portions of the IVC. This interest is due to the fact that one can amplify an electromagnetic field by causing it to interact appropriately with a structure exhibiting NDR.[9] The authors of Refs. 7 and 5 report observing an NDR section on the IVC of a point MBM structure, but the lifetime of the structure did not exceed a few seconds. The experimental observation of an NDR section on the IVC of a planar barrier structure was

reported in Ref. 10. In this case, however, the three-barrier Al-Al_2O_3-Al-Al_2O_3-Al-Al_2O_3-Al structure was investigated, in which the NDR arose as a result of spatial quantization in the thin metallic aluminum films. Unfortunately, only very weak NDR was obtained.

The facts presented above permit the conclusion that it is now appropriate to construct and investigate multibarrier MBM structures with the goal of obtaining NDR regions in their IV curves and the ultimate goal of producing a tunable electromagnetic-radiation generator of a new type.

2. NEGATIVE DIFFERENTIAL RESISTANCE IN TWO-BARRIER MBM STRUCTURES. THEORY

We suggest using a two-barrier planar structure with the barriers separated by a thin metallic layer (Fig. 1) to achieve NDR. When the potential V is applied to the first barrier, the Fermi level of the first metallic layer will shift from its initial position by the amount eV. A nonequilibrium distribution of electrons in the second metallic layer will arise as a result of tunneling through the barrier. It is very important that the energies of the tunneling electrons will lie in a narrow region near the energy $E = \varepsilon_F + eV$. The shape of the energy distribution can be qualitatively explained as follows: there are virtually no electrons above the Fermi lev-
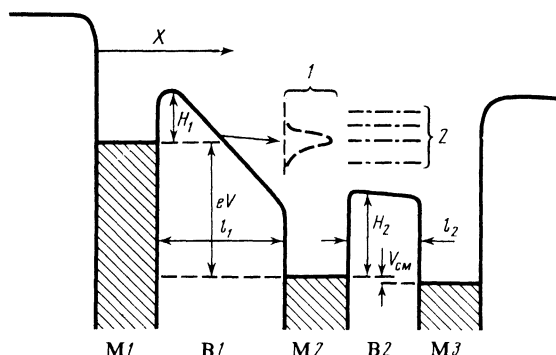

FIG. 1. Energy diagram of a two-barrier MBM structure: 1—distribution of tunnel electrons, 2—transmission resonances, H_1 and H_2—effective heights of the first and second barriers, V_b—bias voltage on the second barrier

el in metal 1, while the tunneling probability for electrons below the Fermi level is small because as an electron recedes from the Fermi level 1) its energy decreases, and 2) the effective thickness of the barrier for that electron increases. We note that an energy distribution of that type for tunneling electrons has been experimentally investigated in Ref. 11.

Let the thickness of the metal be smaller than the mean free path of the electrons within it, so that the electrons will reach the second barrier without losing their narrow energy distribution, and let special measures be taken to ensure the presence of a distinguished direction for the motion of the electrons through the second barrier (e.g., a small bias potential $V_b \ll H_2/e$ may be applied so that the second barrier will be slightly distorted). Then if the potential on the first barrier is high enough ($V > H_2/e$, see Fig. 1) the peak of the energy distribution (1 on Fig. 1) will extend into the region above the second barrier. It is known[12] that the transmission coefficient T_{B2} of a square barrier is not a monotonic function of the incident-particle energy when that energy exceeds the barrier height. T_{B2} becomes unity at certain energy values E_n that we shall call transmission resonances ($T_{B2} < 1$ at intermediate energies). The transmission resonances (2 on Fig. 1) modulate the current through the second barrier: the current is weaker in an interresonance region and is stronger near a transmission resonance. The alternating rise and fall of the current in accordance with the behavior of T_{B2} is what gives rise to NDR segments of the IVC.

We have calculated the IVC of a double MBM structure. Write k_{ix} for the x component of the wave vector $\mathbf{k}_i$ of an electron in metal i, m^* for the effective electron mass, and $E_{ix} = \hbar^2 k_{ix}^2/2m$. Then the transmission coefficient for barrier 1 is given as a function of the energy E_{2x} of an electron in metal 2 and the voltage V by the formula

$$T_{B1}(E_{2x}) = \exp\left\{ -\frac{4}{3} k_V l_1 \left(\frac{\bar{H}_2 + eV - E_x}{eV} \right)^{\!3/2} \right\} \quad \text{at} \quad E_x > H_1 + \varepsilon_F \tag{1}$$

$$T_{B1}(E_{2x}) = \exp\left\{ -\frac{4}{3} k_V l_1 \left[\left(\frac{\bar{H}_2 + eV - E_x}{eV} \right)^{\!3/2} - \left(\frac{\bar{H}_1 - E_x}{eV} \right)^{\!3/2} \right] \right\}$$

at $E_x < H_1 + \varepsilon_F$,

where

$$\bar{H}_i = H_i + \varepsilon_F \quad (i = 1, 2), \quad \hbar k_V = (2m^* eV)^{1/2}.$$

The transmission coefficient T_{B2} of barrier 2 is given for the cases of tunneling ($E_{2x} < \varepsilon_F + H_2$) and of passage above the barrier ($E_{2x} > \varepsilon_F + H_2$) by the formulas[12]

$$T_{B2}(E_{2x}) = \frac{E_{2x}(\bar{H}_2 - E_{2x})}{E_{2x}(\bar{H}_2 - E_{2x}) + \bar{H}_2^2 \, \text{sh}^2 \, \varkappa l_2},$$

$$\varkappa = [2m^*(\bar{H}_2 - E_{2x})]^{1/2}/\hbar \quad \text{at} \quad E_{2x} < H + \varepsilon_F, \tag{2}$$

$$T_{B2}(E_{2x}) = \frac{E_{2x}(E_{2x} - \bar{H}_2)}{E_{2x}(E_{2x} - \bar{H}_2) + \bar{H}_2^2 \sin^2 q l_2},$$

$$q = [2m^*(E_{2x} - \bar{H}_2)]^{1/2}/\hbar \quad \text{at} \quad E_{2x} > H_2 + \varepsilon_F.$$

Since we are interested in effects associated with above-barrier passage of electrons across barrier 2, and this takes place when $eV \gtrsim H_2$, the main contribution to the current through the structure comes from electrons passing from the

left to the right (see Fig. 1). In this case the current density J can be written in the form[2]

$$J = e \int_0^\infty dk_{1x} \int_{-\infty}^\infty dk_{1y} \int_{-\infty}^\infty dk_{1z} \frac{2}{(2\pi\hbar)^3} v_{1x} f(E_1) T_{B1}(E_{1x}) T_{B2}(E_{2x}). \tag{3}$$

Here $e = |e|$ is the electron charge, v_{ix} is the x component of the electron velocity in metal 1, $f(E_1)$ is the Fermi energy distribution in metal 1,

$$f(E_1) = f(E_{1x} + E_{1y} + E_{1z}) = \left\{ 1 + \exp\left[\frac{E_{1x} + E_{1y} + E_{1z} - \varepsilon_F}{kT} \right] \right\}^{-1},$$

ε_F is the Fermi energy of metal 1, and T is the temperature. Integrating over k_y and k_z yields

$$J = e \int_0^\infty dE_{2x} T_{B1}(E_{2x}) T_{B2}(E_{2x}) N(E_{2x} - eV), \tag{4}$$

where

$$N(E_{2x}) = \frac{4\pi m^* kT}{(2\pi\hbar)^3} \ln\left[1 + \exp\left(\frac{\varepsilon_F - E_{2x}}{kT} \right) \right].$$

The product

$$N'(E_{2x}) = T_{B2}(E_{2x}) N(E_{2x} - eV)$$

gives the distribution of the energy E_{2x} of the tunnel electrons in metal 2 after they have crossed barrier 1.

Figure 2 shows the results of computer calculations of $N(E_{2x})$ and $T_{B2}(E_{2x})$. The parameter values used in the calculations are given in the figure caption. It will be seen that the energy distribution of the electrons is rather narrow; its full width Δ_1 can be estimated from the formula

$$\Delta_1 = \frac{2.7}{l_1} \frac{V}{H_1^{1/2} - (H_1 - V)^{1/2}}, \tag{5}$$

where Δ_1, H_1, and H_2 are in electron volts, l_1 is in ångströms, and V is in volts. It is also evident that T_{B2} is an oscillating function of E_{2x} when $E_{2x} > H_2$. The separation Δ_2 between the maxima n and $n + 1$ of the function $T_{B2}(E_{2x})$ is given by the expression

$$\Delta_2 = \frac{3.75}{l_2^2}(2n+1), \quad n = 1, 2, 3, \ldots, \tag{6}$$

in which Δ_2 is in electron volts and l_2 is in ångströms. The condition that the IVC of a double structure be nonmonotonic is obviously that

$$\Delta_2 \gtrsim \Delta_1. \tag{7}$$

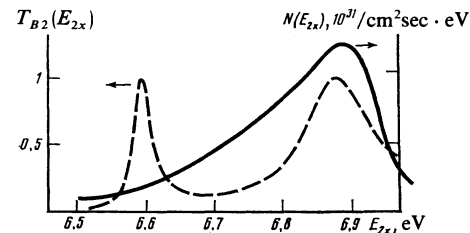FIG. 2. Calculated $N(E_{2x})$ and T_{B2} distributions. The values of the structure parameters used in the calculation were $l_1 = 25$ Å, $H_1 = 2.5$ eV, $V = 2$ V, $\varepsilon_F = 5eV$, and $T = 77$ K for $N(E_{2x})$ and $l_2 = 30$ Å, $H_2 = 1.5$ eV, and $\varepsilon_F = 5$ eV for T_{B2}.
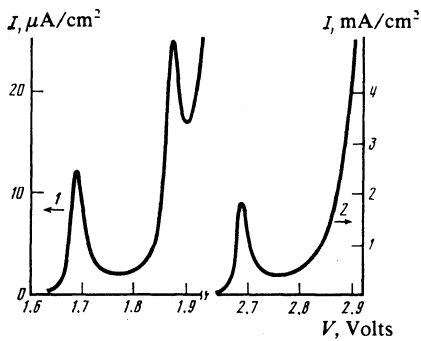
FIG. 3. Current-voltage characteristics calculated for the following parameter values: $l_1 = 20$ Å, $H_1 = 3$ eV, $l_2 = 30$ Å, $H_2 = 1.5$ eV, $\varepsilon_F = 5$ eV, and $T = 77$ K for curve 1, and $l_1 = 50$ Å, $H_1 = 1.5$ eV, $l_2 = 30$ Å, and $H_2 = 2.5$ eV for curve 2 (optimized).
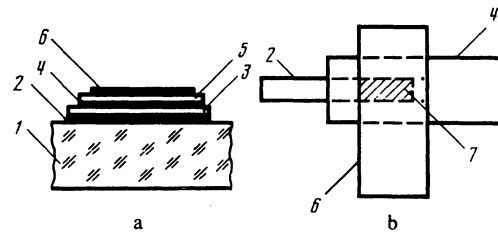

FIG. 4. Experimental two-barrier MBM structure: a) schematic section of the working region, b) general form of the deposited structure; 1—quartz substrate, 2—gold film, 3—MgO film, 4—aluminum film, 5—aluminum oxide film, 6—aluminum film, 7—working region.

Figure 3 shows two IV curves calculated for the structure using two different sets of parameter values. The first parameter set (curve 1) had the structure described in Sec. 3. Current peaks can be seen at 1.68 and 1.88 V.

In the calculation one can vary the parameters l_1, H_1, l_2, and H_2 to optimize the structure from the point of view of increasing the current density in the first (narrowest) current peak. In particular, a structure for which $H_1 \leqslant H_2$ was examined. The nonequilibrium electrons in the second metal have a narrower distribution in this case since they tunnel through the triangular vertex of the first barrier (see Fig. 1): as the electron energy E_1 decreases the tunneling probability decreases even more because of the increase in the effective barrier thickness. This makes it possible to admit more electrons with a narrower energy distribution into the second metal without substantially increasing the total barrier thickness (and thus without increasing the barrier resistance). Curve 2 on Fig. 3 shows the IVC for this case.

It will be seen that the first current peak appears at $V = 2.69$ V, while the current itself amounts to 1.8 mA/cm². Thus, by optimizing the parameters the current can be increased by more than two orders of magnitude.

3. EXPERIMENTAL RESULTS ON THE NDR OF A TWO-BARRIER STRUCTURE

Figure 4 is a schematic representation of the investigated two-barrier structure. The structure was prepared as follows. An Au layer (2) was deposited on the quartz substrate (1) by vaporization and the Au layer was coated with MgO by deposition from solutions. The thickness of the MgO layer was monitored by ellipsometry and amounted to 35 Å. A thin Al layer (4) was deposited on the surface of the dielectric and was then oxidized by an electrical discharge in oxygen at 2×10^{-2} Torr to obtain an Al_2O_3 layer (5) with a calculated thickness of about 20 Å. This layer was covered by a third layer of aluminum (6). The thickness of the second metallic layer turns out to have a substantial effect on the operating capability of the structure since it is that layer that the monoenergetic electron beam passes through. It has been pointed out elsewhere[13] that the thermalization length for the Al that was used in our experiments amounts to 100 Å. In the experimental structures, the second metallic layer was deposited to

a thickness of 100 Å. The oxidation of this layer to produce the second barrier reduced its thickness to 85–90 Å. Considerable technical complications are encountered in an attempt to produce thinner metallic layers. The second barrier was produced, i.e., the layers 4, 5, and 6 were deposited, without breaking the vacuum in order to minimize the uncontrollable interaction of the surfaces of the films with the atmosphere. The electrode configuration (Fig. 4,b) was such that no shunting contact could develop between the electrodes 2 and 6.

The electrical circuit for the experimental setup for investigating NDR is shown schematically in Fig. 5. In this setup the dc component of the current was compensated in order to be able to measure slight changes in the resistance of the MgO barrier (5) due to changes in the energy of the electrons incident on it, i.e., actually to changes in the voltage V across the first barrier (2). To do this a bias voltage $V_b = 20$ mV was applied to the second barrier (5) with the aid of the current source (8) and the variable resistor (6). The compensating voltage was supplied by the type R306 low-resistance potentiometer. The sensitive current input Y (4) of a type F-359 X-Y plotter was connected between the point c and the positive output of the R306 potentiometer, these two points having the same potential under compensation conditions. The potential across the first barrier between the points a and b was fed to the X input (3) of the plotter. Thus, the system made it possible to record changes in the current I_{bc} through the second barrier (between points b and c) due to changes in the voltage V across the first barrier. An Al-
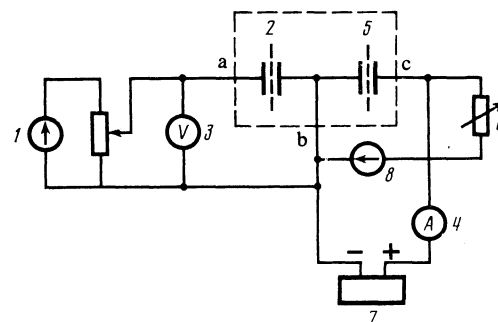

FIG. 5. Experimental setup: 1—voltage source, 2—first barrier, 3—voltage input (X axis of the X-Y plotter), 4—current input (Y axis of the X-Y plotter), 5—second barrier, 6—type R303 resistance box, 7—type R306 potentiometer, 8—second-barrier bias source.
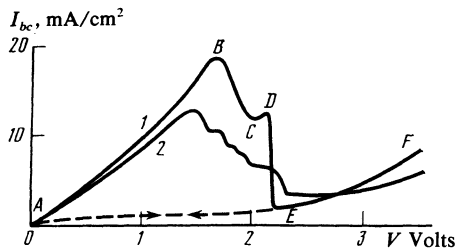
FIG. 6. Experimental curves of the current I_{bc} through the second barrier vs the bias voltage V on the first barrier: 1—$T = 300$ K, 2—$T = 77$ K.

Al_2O_3-Al barrier was used as an emitter of monoenergetic electrons.

Curve 1 in Fig. 6 is a typical experimental graph of I_{bc} vs V. Five different regions of the graph that exhibit characteristically different behaviors of the IVC of the structure can be distinguished: AB (0–1.6 V), BC (1.6–1.9 V), CD (1.9–2.4 V), DE (2.1–2.3 V), and EF (2.3–3.3 V).

The current on the portion AB of the curve is due to monoenergetic electrons tunneling through the sceond barrier and partially passing over it. The decrease in the current on the section BC is due to the peak of the energy distribution of the nonequilibrium electrons passing through a transmission-resonance region, so the section BC corresponds to a portion of the NDR structure; moreover, the 8-μA decrease in the current observed here amounts to 5% of the total current through the second barrier (i.e. the bias current plus the maximum change in the current at point B). The slight rise of the current on section CD corresponds to an increase in the resistance of the second barrier, in other words, to the tunnel electrons' leaving the transmission-resonance region.

The sharp decrease in the current at 2.1 V (point D) is associated with the destruction of the thin second conducting metallic layer as a result of the sharp rise in the current through it due to the reflection of tunnel electrons from the second barrier as they leave the transmission resonance region (at point b on the diagram). As a result, the source 1 (Fig. 5) comes to be connected to series with the R306 potentiometer, which has a high internal resistance. In this case the compensation circuit was actually disconnected and what was measured was the IVC of two successive barriers in series with the resistance of the R306 bridge. The dashed curve in Fig. 6 shows the behavior in subsequent measurements made after the structure was ruptured. It is important that in repeated measurements on this structure up to the rupture point (C) the peak current remains unchanged. This fact favors the thesis that the presence of an NDR section is not due to any sort of degredation.

The curves discussed above were recorded at 300 K. Curve 2 in Fig. 6 was recorded similarly, but at 77 K. It will be seen that the voltage at which I_{bc} reaches its maximum is almost the same at 77 K as at 300 K. The small difference can perhaps be attributed to the temperature dependence of the barrier parameters. This again confirms the tunnel mechanism for the operation of the investigated two-barrier structure.

As was mentioned above, scattering of electrons in the second metallic layer was not taken into account in calculating the IVC. Such scattering does take place, and it leads to broadening of the energy distribution of the monoenergetic electron beam. As is evident from the calculations (see Fig. 2), the half-width of the electron distribution is of the same order as the separation between the levels. This broadening of the distribution as a result of partial thermalization of the electrons may make it impossible to resolve the first and second transmission-resonance peaks. An attempt to reduce the thermalization by making the second metallic layer even thinner encounters considerable technical difficulties associated with the deposition of high-quality metallic layers less than 100 Å thick. In addition, the Ohmic resistance of such thin layers would result in greater evolution of heat and rapid degradation of the structure.

4. ON THE POSSIBILITY OF USING MBMBM STRUCTURES TO CONSTRUCT A FREQUENCY-TUNABLE OPTICAL GENERATOR

An illustration of the validity of the physical mechanism considered for the NDR in a dual MBMBM structure is the generation in such structures of radio-frequency electromagnetic radiation, which was first observed by the present authors.[14] In that experiment we used an Al-Al_2O_3-Al-Al_2O_3-Al structure with layer thicknesses of 500, 30, 90, 30, and 300 Å, respectively, the dielectric layers being formed by oxidation in a high-voltage discharge in oxygen at 2×10^{-2} Torr. The generated frequency was 180 kHz and was tunable through 30 kHz; moreover, oscillation occurred only when the potentials on the structure corresponded unambiguously to an NDR section on the IVC.

As we noted in the introduction, according to experiments on detecting optical emission and frequency multiplication and mixing,[1] metal-barrier-metal tunnel structures have very short response times down to 10^{-14}–10^{-15} sec; hence the static IVC of such a structure will be valid even at optical frequencies. This permits us to assume that the IVC of an MBMBM structure such as those described above, including its NDR protion, will also be applicable in the optical region. If this is the case, one can use such structures to amplify and generate electromagnetic radiation in the optical region. Below we calculate the characteristics of a generator based on an MBMBM structure.

Let us consider a system of N MBMBM junctions mounted in an optical resonator at the points $r_1, r_2, \ldots, r_N$. In the case of single-mode generation, the field $E(r, t)$ can be expressed in the form $E(r, t) = A(t) \cos(\omega t + \varphi(t))U(r)$, where $U(r)$ is the field distribution in space. One can derive the following equations for the slow variables $E(t)$ and $\varphi(t)$ from Maxwell's equations in the usual manner[15]:

$$\mu W \left(\dot{E} + \frac{1}{\tau} \right) \omega = 4\pi \left\langle \sin(\omega t + \varphi) \frac{\partial}{\partial t} \int_W dr J U(r) \right\rangle,$$

$$\mu W (\dot{\varphi} E) \omega = 4\pi \left\langle \cos(\omega t + \varphi) \frac{\partial}{\partial t} \int_W dr J U(r) \right\rangle,$$

(8)

where the angle brackets indicate averaging over the period of the field oscillations, τ is the dwell time in the resonator, J

is the current density, W is the volume of the resonator, ω is the natural frequency of the resonator, and μ is the value of $u^2(r)$ averaged over the volume of the resonator.

The potential V_i at the point $\mathbf{r}_i$ of the MBMBM junction can be expressed in the form

$$V_i = V + dU(\mathbf{r}_i)A(t).$$

Here V is the constant bias voltage and d is the characteristic size of the contact. In what follows we shall assume that the junction is biased on an NDR section of the IVC. Then the current I_i at the i-th structure can be written as

$$I_i = I[V + dU(V_i)A(t)]$$
$$\approx I(V) - dU(\mathbf{r}_i)A(t)/R_d + kd^3U^3(\mathbf{r}_i)A^3(t), \quad (9)$$

where we have used the expansion of the static current-voltage characteristic $I(V)$ of the structure to terms of the third order in $[dU(\mathbf{r}_i)A(t)]$. The values of the negative differential resistance R_d and the coefficient k were determined from the IVC (see Fig. 6). In what follows we shall assume for estimates that $R_d = V_M/I_a$ and $k = I_a/6V_M^3$, where I_a is the current drop on the NDR portion of the IVC and V_M is the voltage interval in which NDR appears. On substituting (9) into (8) we obtain the following set of equations for the amplitude and phase of the genrated radiation:

$$\dot{E} + E/\tau = (2\pi/\mu W)[R_d^{-1}Nd^2\overline{U}_i^2 - {}^3/_4kNd^4\overline{U}_i^4E^2]E, \quad (10)$$

$$\mu W\dot{\varphi}E = 0, \quad (11)$$

where

$$\overline{U}_i^k = \frac{1}{N}\sum_i U^k(\mathbf{r}_i), \quad k = 2, 4.$$

In deriving Eqs. (10) and (11) we took account of the fact that the following relation is satisfied at the i-th junction.

$$\int_W d\mathbf{r}J_i(\mathbf{r})U(\mathbf{r}_i) = U(\mathbf{r}_i)I_id,$$

where $J_i(\mathbf{r})$ is the current density produced by the i-th junction. We note that Eqs. (10) and (11) are similar to those for a gaseous laser.[15]

It is evident from Eq. (11) that the phase φ is constant, while the stationary solution of Eq. (10) has the form

$$E^2 = \frac{R_d^{-1}Nd^2\overline{U}_i^2 - (\mu W/2\pi\tau)}{3kNd^4\overline{U}_i^4/4}. \quad (12)$$

As is evident from Eq. (10), the generation threshold is determined by the equation

$$R_d^{-1}Nd^2\overline{U}_i^2 = \mu W/2\pi\tau \quad (13)$$

and is independent of frequency. The frequency independence is associated with a simplification of the model which, in any case, does not take account of the limiting time lag of the MBMBM structure.

It follows from Eq. (13) that the negative resistivity of the structure, $\rho_d = R_dS/d$ (S is the area of the structure), required to achieve generation should satisfy the relation

$$\rho_d < 2\pi\tau(W'/W), \quad (14)$$

where W' is the volume of the resonator occupied by structures exhibiting NDR and $W' = NSd$. Assuming for estimates that $\tau \sim 10^{-8}$ sec, we find that for an element with $S = 1$ cm^2, R_d should at least be smaller than 10 ohms. MBMBM structures with NDR of such values can be obtained by suitble choice of the thicknesses of the dielectric layers.[16]

The power radiated by such a structure can be estimated from the equation $P_{out} = E^2W/4\pi\tau$, where E^2 is given by Eq. (12).

When operating considerably above the threshold, we have $E^2 \sim V_M^2/d^2$. Assuming that $W \sim 10^{-1}$–10^0 cm^2, $\tau \sim 10^{-8}$ sec, and $V_M \sim 10^{-4}$ V, we find that $P_{out} \sim 10$–100 mW. It is evident from these estimates that it will be possible in principle, under realistic experimental conditions, to construct generators that will be tunable over the entire frequency range of the spectrum, the frequency tuning being achieved by varying the resonator frequency ω. We note that such generators can be very small, so it will be possible to use them in integrated optical circuits.

[1]V. M. Klement'ev, Yu. A. Matyugin, and V. P. Chebotaev, Kvant. Elektron. (Moscow) 5, 1671 (1978) [Sov. J. Quantum Electron. 8, 953 (1978)].
[2]In: Tunnel'nye yavleniya v tverdykh telakh (Tunneling Phenomena in Solids), transl. coll., Mir, Moscow, 1973, p. 38.
[3]H. D. Riccius, Appl. Phys. 17, 49 (1978).
[4]J. G. Small, G. M. Elchinger, et al., Appl. Phys. Lett. 24, 275 (1974).
[5]É. M. Belenov, S. I. Vedeneev, and A. V. Uskov, Kvant. Elektron. (Moscow) 8, 163 (1981) [Sov. J. Quantum Electron. 11, 91 (1981)].
[6]R. K. Jain, Sigurd Wagner, and D. H. Olsson, Appl. Phys. Lett. 32, 62 (1978).
[7]In Ref. 2, pp. 25–35 and 223–232.
[8]Thomas E. Hartman, J. Appl. Phys. 33, 3427 (1962).
[9]D. Drury and T. Ishii, IEEE Trans. on Microwave Theory and Technique, MTT-27, 602 (1979).
[10]Sadao Takabe, Kanji Yasui, and Shiego Kaneda, Appl. Phys. Lett. 31, 636 (1977).
[11]H. Kanter and W. A. Feibelman, J. Appl. Phys. 33, 3580 (1962).
[12]L. D. Landau and E. M. Lifshitz, Teoreticheskaya fizika, t. 3 (Theoretical physics, Vol. 3), Fizmatgizdat., Moscow, 1963, pp. 103–104 Engl. Transl. Quantum mechanics, Nonrelativistic Theory, Pergamon.
[13]S. M. Sze, C. R. Crowell, G. P. Carrey, and E. E. La Bate, J. appl. Phys. 37, 2690 (1966).
[14]A. G. Aleksanyan, E. M. Velenov, I. N. Kompanets, Yu. M. Popov, I. A. Poluéktov, A. G. Sobolev, A. V. Uskov and V. G. Tsukanov, Kvantovaya Elektron. (Moscow) 9, 1463 (1982) [Sov. J. Quantum Electron. 12, 930 (1982)].
[15]W. E. Lamb Jr., Theory of an optical maser, Phys. Rev. 134, A1429–A1450 (1964).
[16]A. G. Aleksanyan, É. M. Belenov, I. N. Kompanets, Yu. M. Popov, I. A. Poluéktov, S. I. Sagitov, E. M. Soboleva, A. G. Sobolev, E. P. Turevskaya, I. Ya. Turova, A. V. Uskov, V. G. Tsukanov, and M. I. Yanovskaya, FIAN reprint No. 132, 1981.

Translated by E. Brunner